First-principles studies of the geometry and energetics of the Si_{36} cluster

Q. Sun,[1,2] Q. Wang,[1,2] P. Jena,[2] S. Waterman,[3] and Y. Kawazoe[1]
[1]*Institute for Materials Research, Tohoku University, Sendai 980-77, Japan*
[2]*Physics Department, Virginia Commonwealth University, Richmond, Virginia 23284, USA*
[3]*2555 Benny 1105, NDG, Montreal Quebec, Canada H4B 2R6*
(Received 15 August 2002; revised manuscript received 16 December 2002; published 10 June 2003)

First-principles studies of the geometry and energetics of the Si_{36} cluster are performed by searching 17 structural isomers including cage, wire, and stuffed fullerene. It is found that the tricapped-trigonal-prism unit is not the structural unit for Si_{36}, and the stable structure is identified to have a more spherical geometry derived from the stuffed fullerene configurations. This is in agreement with the experiment which suggested a structural transition from the elongated geometry to a more spherical one for the medium sized silicon cluster [Hudgins *et al.*, J. Chem. Phys. **111**, 7865 (1999); Bergeron *et al.*, J. Chem. Phys. **117**, 3219 (2002)].

DOI: 10.1103/PhysRevA.67.063201 PACS number(s): 36.40.Cg, 61.46.+w, 71.20.Tx, 61.48.+c

I. INTRODUCTION

In recent years, with the advent of flexible and precise experimental techniques, the well-controlled small carbon clusters became experimentally accessible, such as C_{20} [1–4], C_{28} [5], and C_{36} [6–14]. C_{20} is the smallest fullerene cage [3,4], and C_{28} together with C_{20} is the structural unit of carbon clathrates. Especially C_{36} can form stable cluster assembled materials with novel properties [6–14]. The rich structures and interesting properties of carbon fullerenes have fueled parallel studies of Si clusters, not only because carbon and silicon are members of the same group in the periodic table, but more importantly silicon has great potential applications in computer chips, microelectronic devices, catalysts, and new superconducting compounds. Recently, Si_{20} [15–20], Si_{28} [21], and Si_{60} [22–32] clusters have been investigated. It is well established that C_{20} has dodecahedron cage structure, while Si_{20} has a wirelike structure composed of two Si_{10} units. Similarly, Si_{28} also has a wire structure composed of tricapped-trigonal-prism (TTP) units [21]. On the other hand, Si_{60} prefers to form a more compact structure [32]. In this paper, we study the structure and energetics of the Si_{36} cluster, which is motivated by the following two points:

(1) TTP units are found to be the structural building blocks for Si_{20} and Si_{28}. A determination, as to the validity of TTP units as building blocks of Si_{36}, is quite important towards a more complete understanding of silicon structural growth.

(2) Experimental studies of the chemical reactions of size-selected silicon clusters with ammonia [33] found that the largest equilibrium reaction constants existed for the Si_{36} cluster. Although more than 10 years had passed since this experiment, to the best of our knowledge, no explanation has been given for this reactivity experiment. It is known that reactivity of a cluster is intimately related to its electronic structure, while the latter is sensitively dependent on its geometry. Therefore, the determination of the geometry of Si_{36} would be the first step to understand its reactivity.

II. COMPUTATIONAL METHOD

In this paper, we have used density-functional theory [34,35]. For the exchange-correlation functional, gradient-corrected functionals in the form of the generalized gradient approximation [36] have been chosen. In order to optimize geometry effectively, a plane-wave basis set is adopted with the projector-augmented wave (PAW) method originally developed by Blöchl [37] and recently adapted by Kresse and Joubert [38]. The particular advantage of the PAW method over the ultrasoft pseudopotentials is that it can improve accuracy, especially in those cases where the overlap between the valence- and the core-charge densities and hence the nonlinearity of the core-valence exchange are important. In our calculations, the cluster is placed in a cubic cell with edge length of 30 Å, which is sufficiently large to make dispersion effects negligible. In such a big supercell, only the Γ point can be used to represent the Brillouin zone. The plane-wave cutoff is 300 eV, which is found to be large enough to get a good convergence. The structure optimization is symmetry unrestricted, and conjugate-gradient algorithm has been chosen. The optimization is terminated when all the forces acting on the atoms are less than 0.01 eV/Å.

III. RESULTS AND DISCUSSION

Knowledge of the geometrical structure of clusters is essential to understand their physical and chemical properties. However, obtaining the ground-state geometry of a large cluster is not a trivial task as there are many isomers and the result may depend upon the initial geometry used for optimization. Moreover, the structures of nano-Si are much more complicated than those of carbon although both are in the same group. For example, the pentagon and hexagon are the basic structural units, not only for carbon fullerene cage and carbon nanotube but also for carbon nanohorn. However, for nanosilicon, such a simple structural pattern does not exist. Many studies have been devoted to this subject and several structural models are proposed, including fullerene cage model [39], TTP model [15,16], and stuffed fullerene model [40]. In the recent study, it has been found that 8-atom units and 6-atom units are important for the large Si cluster [41]. Based on these findings, we performed an extensive search for the structure of Si_{36}.

First we consider the cage structures as shown in Fig. 1. Cage 1 is a fullerene cage with D_{6h} symmetry, which is found to be the ground-state geometry for C_{36} [7], as shown

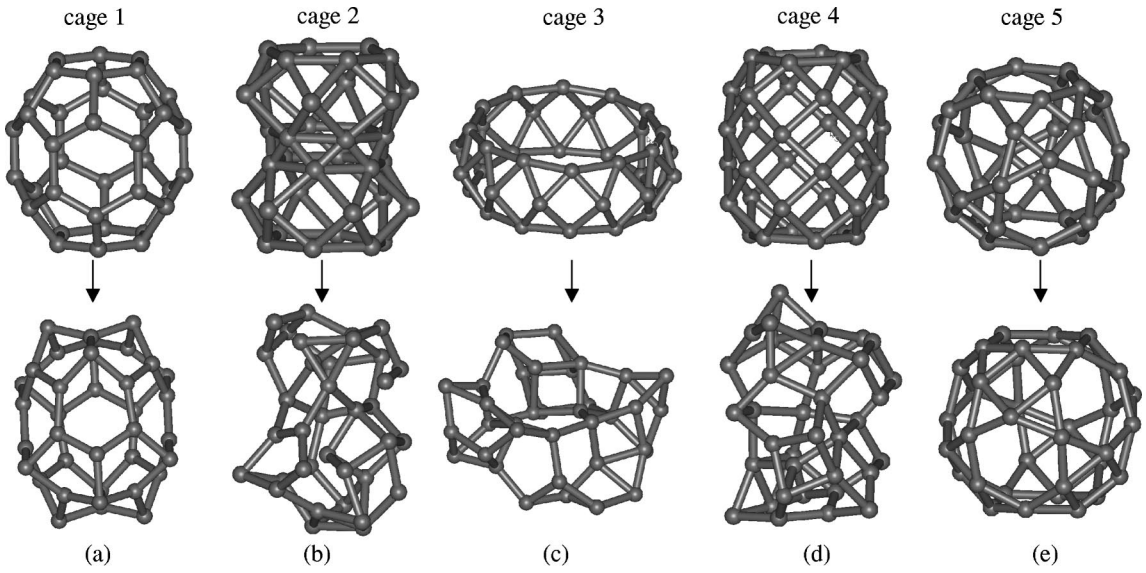

FIG. 1. The initial and optimized geometries of Si_{36} confined to different cage structures.

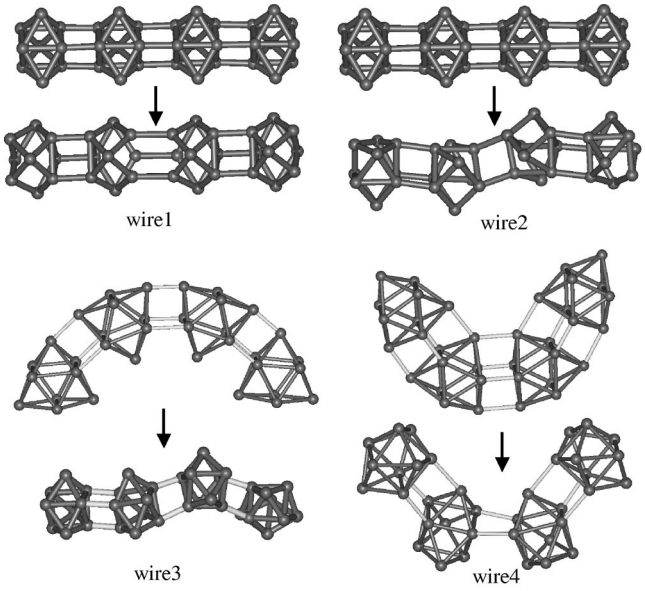

FIG. 2. The initial and optimized geometries of Si_{36} with wire-like structure composed of TTP units as building blocks.

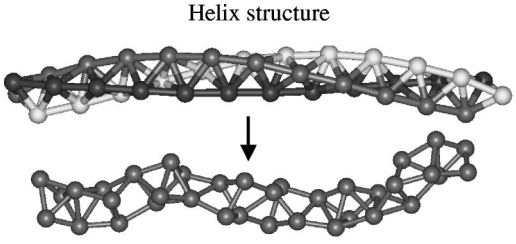

FIG. 3. The starting and optimized helix structures for Si_{36}.

in Fig. 1(a). Cage 2 consists of Si_{18} dimer where each atom in Si_{18} has coordination number of four [Fig. 1(b)]. Cage 3 is composed of three Si_{12} rings where each Si atom is fourfold coordinated [Fig. 1(c)]. While six Si_6 rings construct cage 4 [Fig. 1(d)], each Si atom is also fourfold coordinated. Cage 5 is Waterman cage with O_h symmetry, composed of 6 squares, 24 triangles, and 8 hexagons [Fig. 1(e)]. When fully optimized, the cage structures can be kept for cages 1 and 5,

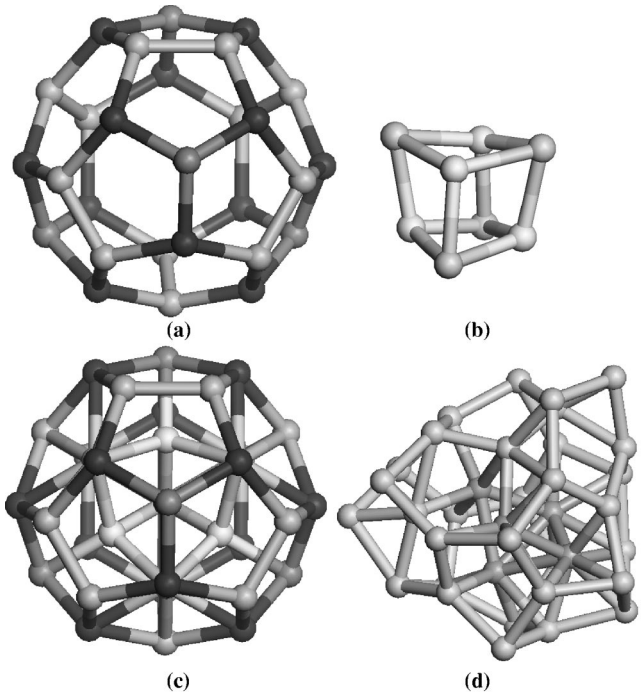

FIG. 4. The stuffed-fullerene structure (Stuff28-*A*). (a) Si_{28} fullerene cage with T_d symmetry. (b) The 8-atom core with T_d symmetry that could be encapsulated into Si_{28}. (c) The initial stuffed cage for Si_{36} with T_d symmetry. (d) The optimized structure of Si_{36}.

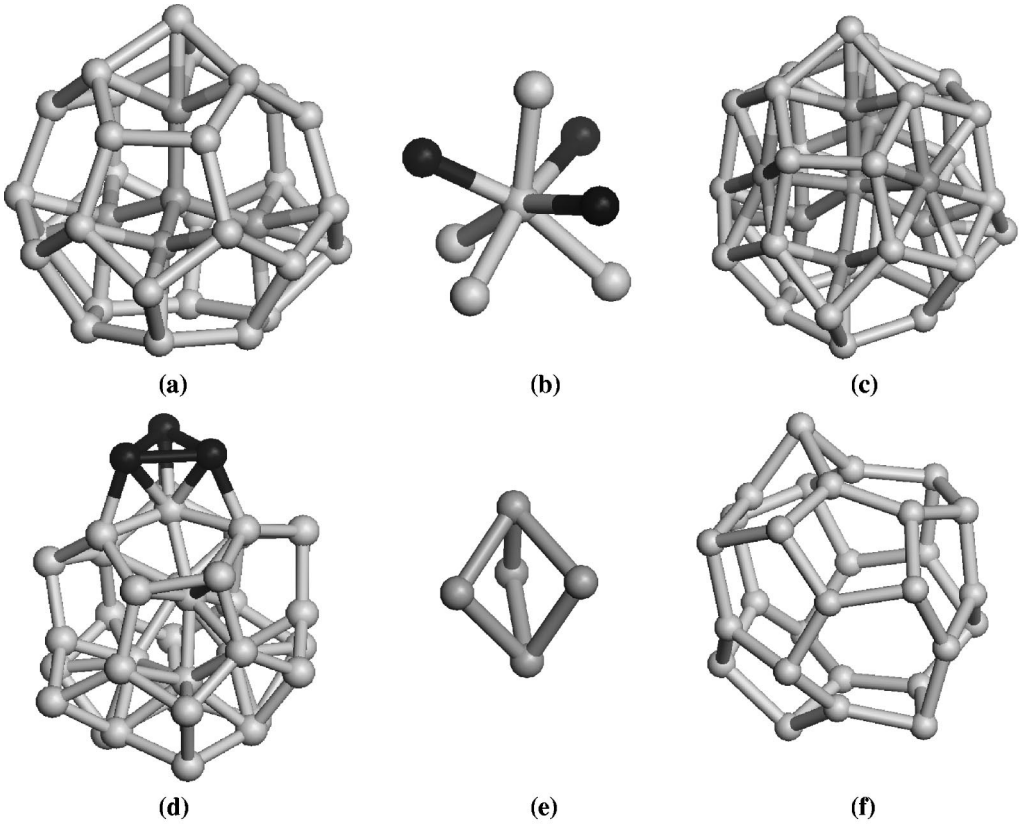

FIG. 5. Stuff28-*B* structure. (a) Si_{28+5} fullerene cage. (b) The 8-atom core by adding three atoms to 5-atom unit. (c) The initial stuffed cage with C_{3v} symmetry. (d) The optimized structure where three atoms (in black) are squeezed out from the core and bonded on the cage surface. (e) The optimized core. (f) The second shell cage.

while the other three cages are seriously destroyed.

Next we consider the wire structure. Here, the basic reason is that tricapped trigonal prisms Si_9 is found to be the stacking unit [15,16], and Si_{36} may contain four such stacking units. However, there are several ways to assemble these four units, as shown in Fig. 2. In wire 1, the four units are stacked strictly along one line, the structure can keep the symmetry when fully optimized. In wire 2, the four units are shifted off the line, and the final structure becomes distorted wire with lower energy. In wire 3, the four units form an arclike structure, but the final structure becomes wirelike again. By increasing the curvature, we get wire 4, however, its energy becomes higher. As for the wire structure, we also have another candidate, the Boerdijk-Coxeter helix structure, as shown in Fig. 3, which is a linear stacking of regular tetrahedrons. Helices and dense packing of spherical objects are two closely related problems, and the Boerdijk-Coxeter helix structure is most close-packed for one-dimensional system [42]. However, due to the covalent bonding features of silicon atoms, the optimized structure is seriously distorted with much higher energy.

Finally, we study the stuffed fullerene structure. The best example of the Si cluster with stuffed fullerene structure is Si_{33} [40], which is composed of Si_{28} and Si_5. Here, we have several options for the stuffed structures of Si_{36}: Si_{28+8}, Si_{30+6}, Si_{32+4}, and Si_{34+2}. However, for the last two cases, 4-atom core and 2-atom core are too small for Si_{32} cage and Si_{34} cage, respectively. Therefore, we consider only the first two cases to encapsulate 8-atom unit and 6-atom unit, which are important units for the large Si cluster [41].

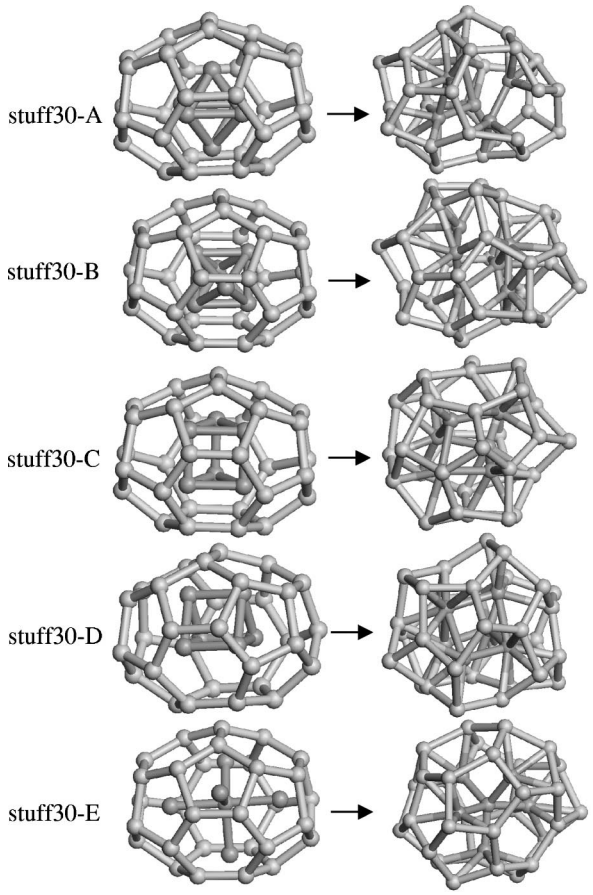

FIG. 6. The initial and optimized structures for stuff30 configurations.

TABLE I. Total binding energy E (in eV) and HOMO-LUMO gap (in eV) for the 17 isomers considered. The last column lists the symmetries of the initial and optimized ones.

Isomer	E	HOMO-LUMO	Symmetry
Cage 1	139.406	0.657	$D_{6h}\rightarrow D_{3d}$
Cage 2	140.680	0.488	$C_{6v}\rightarrow C_1$
Cage 3	139.603	0.597	$D_{12h}\rightarrow C_1$
Cage 4	140.328	0.550	$D_{6v}\rightarrow C_1$
Cage 5	127.236	0.045	$O_h\rightarrow O_h$
Wire 1	141.632	0.075	$C_{3h}\rightarrow C_{3h}$
Wire 2	142.776	0.532	$C_1\rightarrow C_1$
Wire 3	141.834	0.657	$C_2\rightarrow C_1$
Wire 4	142.490	0.716	$C_2\rightarrow C_1$
Helix	137.003	1.010	$C_1\rightarrow C_1$
Stuff28-*A*	142.986	0.651	$T_d\rightarrow C_1$
Stuff28-*B*	143.347	0.331	$C_3v\rightarrow C_1$
Stuff30-*A*	143.730	0.469	$C_2\rightarrow C_1$
Stuff30-*B*	143.290	0.224	$C_2v\rightarrow C_1$
Stuff30-*C*	143.457	0.501	$C_s\rightarrow C_s$
Stuff30-*D*	143.904	0.552	$C_s\rightarrow C_1$
Stuff30-*E*	143.234	0.712	$C_1\rightarrow C_s$

1. *Stuffed* Si_{28+8} *structures*

We know that C_{28} cage with T_d symmetry consists of 12 pentagons and 4 hexagons [Fig. 4(a)]. Now we put Si_8 with T_d symmetry as a core [Fig. 4(b)] inside the cage, the complex cluster also has T_d symmetry [Fig. 4(c)], which is the most symmetric stuffed fullerene structure one could find for Si_{36}, labeled as stuff28-A. We used it as the initial structure, when fully optimized, the cluster is distorted with C_1 symmetry [Fig. 4(d)], the core is broken, and only five atoms stay inside the cage, the other three atoms are squeezed out and joined the outer shell.

There is another way to construct Si_{28+8}, which is equivalent to Si_{28+5+3}. Figure 5(a) shows Si_{28+5}, we can add another three atoms to the core as shown in Fig. 5(b), then we orient the core to make the complex structure having C_{3v} symmetry [Fig. 5(c)]. When fully optimized, the structure becomes onionlike [Fig. 5(d)], labeled as stuff28-B. The first shell is a 5-atom core with triangle bipyramid configuration [Fig. 5(e)], and the second shell is 28-atom cage [Fig. 5(f)]. It is interesting to note that these first two shells correspond to optimized geometry of Si_{33} [40]. In stuff28-*B*, there are three atoms moving out from the core and bind on the surface of Si_{33}, which suggests again that Si_{28} cage is too small to encapsulate Si_8 unit.

2. *Stuffed* Si_{30+6} *structures*

The ground-state geometry for C_{30} is C_{2v} structure [43], which is taken for Si_{30}. We first choose the 6-atom core as an octahedron with two orientations, its C_{4v} axis is parallel and perpendicular to the C_{2v} axis of Si_{30}, resulting in the

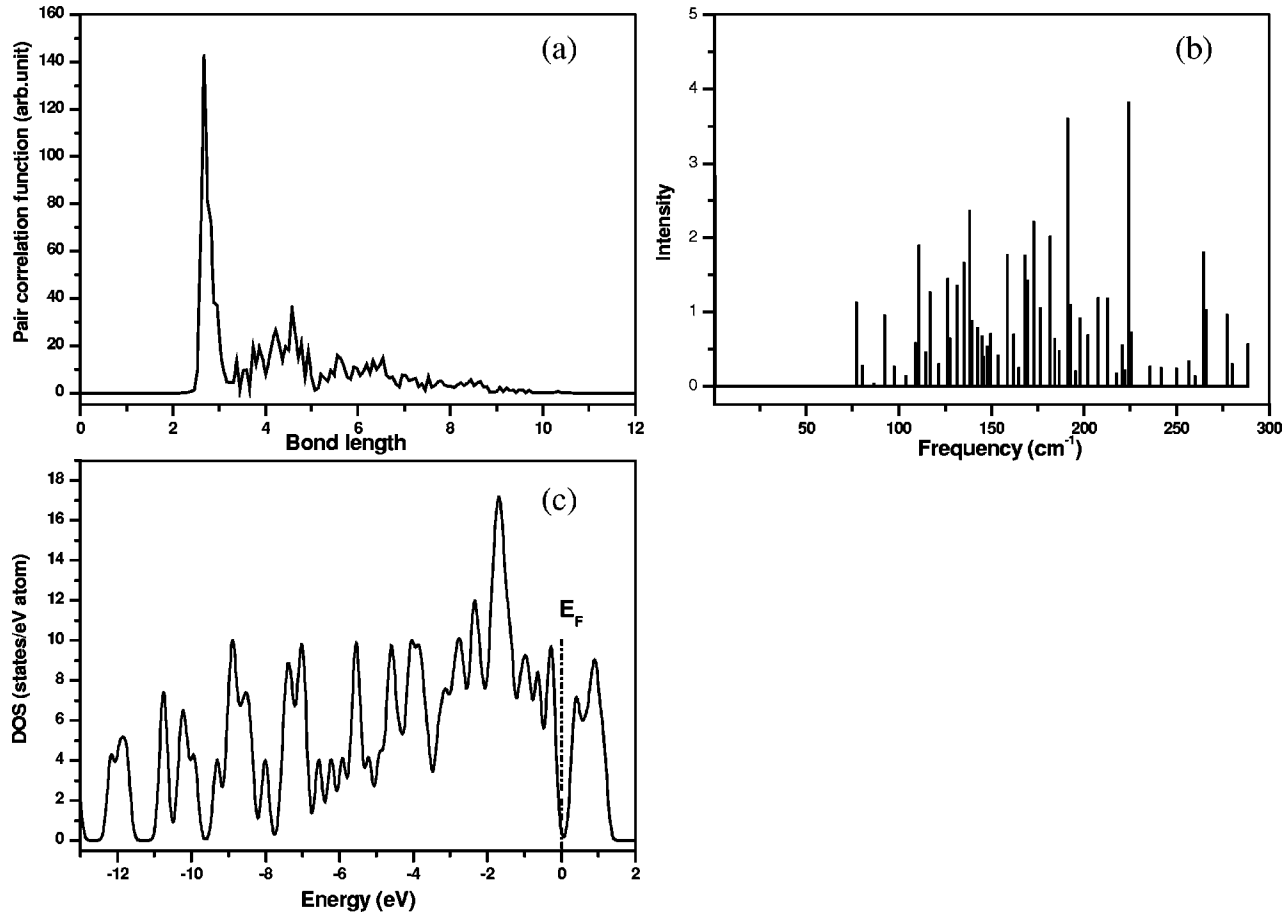

FIG. 7. (a) Pair correlation function, (b) vibrational spectra, and (c) DOS for stuff30-*D* structure in Fig. 6.

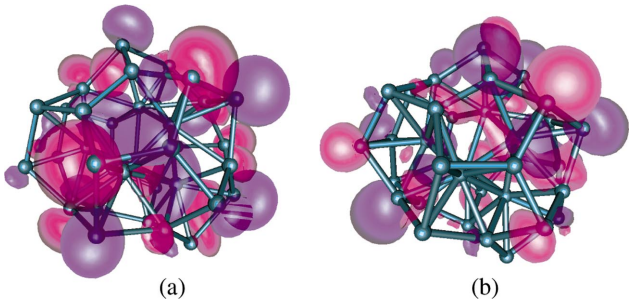

FIG. 8. (Color) (a) The HOMO and (b) LUMO orbitals with the isosurface values of $+0.02$ (in red) and -0.02 (in blue) for stuff30-*D* structure in Fig. 6.

configurations of stuff30-*A* and stuff30-*B*, respectively, in Fig. 6. Similarly, for the core of triangular prism Si_6, its C_{3v} axis is arranged to be parallel and perpendicular to the C_{2v} axis of Si_{30}, which gives the configurations of stuff30-*C* and stuff30-*D*, respectively, in Fig. 6. Finally, we consider Si_6 core with the structure of triangular bipyramid. Due to space limitation of the Si_{30} cage, the C_{3v} axis of core can only be oriented in parallel to the C_{2v} axis of outer cage, labeled as stuff30-*E* in Fig. 6. All the five stuffed fullerene structures are distorted during the geometry optimization. In the first three cases, the cores are destroyed but still being encapsulated inside the cage, while for the last two configurations, the skeletons of the cores are kept.

In Table I, we list the total binding energy, highest occupied molecular orbit-lowest unoccupied molecular orbital (HOMO-LUMO) gap, and the symmetry for all the 17 isomers considered above. Stuff30-*D* structure in Fig. 6 has the lowest energy, about 1.13 eV lower than that of the most stable wire configuration (wire 2 in Fig. 2). We can see that the fullerene cage and TTP unit cannot be used to construct the equilibrium geometry for Si_{36}. Although the wire configuration is more stable than the fullerene cage, the structural transition from the elongated geometry to a more spherical one has already taken place in Si_{36}. This is in agreement with the experimental findings [44,45].

Figure 7 shows more detailed information about the stuff30-*D* structure. The pair correlation function [Fig. 7(a)] suggests that the maximum diameter for this stuffed cage is about 9.5 Å, and the average nearest-neighbor bond length is about 2.3 Å. The stability for this structure is checked by calculating the vibrational spectra, as shown in Fig. 7(b). All the frequencies are real, suggesting that the structure is dynamically stable as well. Figure 7(c) shows the density of states (DOS) with Gaussian broadening of 0.1 eV, the Fermi level is shifted to zero. In order to get some qualitative understanding for the experiment of Si_{36} reacting with ammonia [33], we plot the two frontier HOMO and LUMO orbitals in Figs. 8(a) and 8(b), respectively. We can see that these two frontier orbitals are quite delocalized in space, which suggests that there would be many potential absorption sites on the Si_{36} cluster surface. This may be one of the possible reasons why Si_{36} shows quite a large equilibrium reaction constants when reacting with ammonia [33]. However, a full understanding of this reactivity experiment demands detailed studies, this work is still in progress.

IV. SUMMARY

In summary, we have studied the structure and energetics of the Si_{36} cluster by using first-principles method. We found that stuff30-*D* configuration in Fig. 6 is most stable. This structure has two important features: (1) It is a stuffed fullerene cage. (2) A 6-atom unit is encapsulated, which is found to be an important structural unit for the larger Si cluster. This structure is more stable in energy and more spherical in shape as compared to those of TTP wire. Although the tricapped-trigonal-prism stacking rule is valid for Si_{20} [15,16] and Si_{28} [21], the structural transition from the elongated geometry to more spherical one has taken place in Si_{36}. The delocalized HOMO and LUMO orbitals may result in many potential absorptive sites on this cluster surface, therefore, large equilibrium reaction constants could be expected for some reactions. All these results are in agreement with experiments.

ACKNOWLEDGMENTS

The authors would like to express their sincere thanks to the crew of the Center for Computational Materials Science, the Institute for Materials Research, Tohoku University, for their continuous support of the HITAC SR8000 supercomputing facility.

[1] K. Hata, M. Ariff, K. Tohji, and Y. Saito, Chem. Phys. Lett. **308**, 343 (1999).
[2] G. Galli, F. Gygi, and J. Golaz, Phys. Rev. B **57**, 1860 (1998).
[3] H. Prinzbach, A. Weiler, P. Landenberger, F. Wahl, J. Wrth, L.T. Scott, M. Gelmont, D. Olevano, and B. Issendorff, Nature (London) **407**, 60 (2000).
[4] M.F. Jarrold, Nature (London) **407**, 26 (2000).
[5] D.W. Cox, K.C. Reichmann, and A. Kaldor, J. Chem. Phys. **88**, 1588 (1988).
[6] C. Piscoti, T. Yarger, and A. Zettl, Nature (London) **393**, 771 (1998).
[7] P.G. Collins, J.C. Grossman, M. Ct, M. Ishigami, C. Piskoti, S.G. Louie, M.L. Cohen, and A. Zettl, Phys. Rev. Lett. **82**, 165 (1999).
[8] J.C. Grossman, M. Cote, S.G. Louie, and M.L. Cohen, Chem. Phys. Lett. **284**, 344 (1998).
[9] V. Rosato, M. Celino, S. Gaito, and G. Benedek, Comput. Mater. Sci. **20**, 387 (2001).
[10] G.K. Gueorguiev and J.M. Pacheco, J. Chem. Phys. **114**, 6068 (2001).
[11] M.N. Jagadeesh and J. Chandrasekhar, Chem. Phys. Lett. **305**, 298 (1999).
[12] P.W. Fowler, T. Heine, K.M. Rogers, J.P.B. Sandall, G. Seifert, and F. Zerbetto, Chem. Phys. Lett. **300**, 369 (1999).

[13] V. Rosato, M. Celino, G. Benedek, and S. Gaito, Phys. Rev. B **60**, 16 928 (1999).
[14] J.C. Grossman, S.G. Louie, and M.L. Cohen, Phys. Rev. B **60**, R6941 (1999).
[15] K.M. Ho, A.A. Shvartsburg, B. Pan, Z.Y. Lu, C.Z. Wang, J.G. Wacker, J.L. Fye, and M.F. Jarrold, Nature (London) **392**, 582 (1998).
[16] Jörgen Mller, Bei Liu, Alexandre A. Shvartsburg, Serdar Ogut, James R. Chelikowsky, K.W. Michael Siu, Kai-Ming Ho, and Gerd Gantefor, Phys. Rev. Lett. **85**, 1666 (2000).
[17] J. Wang, J. Zhao, F. Ding, W. Shen, H. Lee, and G.H. Wang, Solid State Commun. **117**, 593 (2001).
[18] L. Mitas, J.C. Grossman, I. Stich, and J. Tobik, Phys. Rev. Lett. **84**, 1497 (2000).
[19] B.X. Li and P.L. Cao, Phys. Rev. A **62**, 23201 (2000).
[20] Q. Sun, Q. Wang, T.M. Briere, V. Kumar, Y. Kawazoe, and P. Jena, Phys. Rev. B **65**, 235417 (2002).
[21] M.F. Jarrold and J.E. Bower, J. Chem. Phys. **96**, 9180 (1992).
[22] M.C. Piqueras, R. Crespo, E. Orti, and F. Tomas, Synth. Met. **61**, 155 (1993).
[23] R. Crespo, M.C. Piqueras, and F. Tomas, Synth. Met. **77**, 13 (1996).
[24] M.C. Piqueras, R. Crespo, E. Orti, and F. Tomas, Chem. Phys. Lett. **213**, 509 (1993).
[25] S. Nagase and K. Kobayashi, Chem. Phys. Lett. **187**, 291 (1991).
[26] S. Nagase, Pure Appl. Chem. **65**, 675 (1993).
[27] Z. Slanina, S.L. Lee, K. Kobayashi, and S. Nagase, J. Mol. Struct.: THEOCHEM **312**, 175 (1994).
[28] F.S. Khan and J.Q. Broughton, Phys. Rev. B **43**, 11 754 (1991).
[29] M. Menon and K.R. Subbaswamy, Chem. Phys. Lett. **219**, 219 (1994).
[30] B.X. Li, P.L. Cao, and D.L. Que, Phys. Rev. B **61**, 1685 (2000).
[31] E.F. Sheka, E.A. Nikitina, V.A. Zaets II, and I.Ya. Ginzburg, JETP Lett. **74**, 177 (2001).
[32] Q. Sun, Q. Wang, P. Jena, B. K. Rao, and Y. Kawazoe, Phys. Rev. Lett. **90**, 135503 (2003).
[33] M.F. Jarrold, Y. Ijiri, and U. Ray, J. Chem. Phys. **94**, 3607 (1991).
[34] W. Kohn and L. Sham, Phys. Rev. A **140**, 1133 (1965).
[35] G. Kresse and J. Furthmüller, Comput. Mater. Sci. **6**, 15 (1996).
[36] J.P. Perdew, J.A. Chevary, S.H. Voksko, K.A. Jackson, M.R. Pedersen, D.J. Singh, and C. Fiolhais, Phys. Rev. B **46**, 6671 (1992).
[37] P. Blöchl, Phys. Rev. B **50**, 17 953 (1994).
[38] G. Kresse and D. Joubert, Phys. Rev. B **59**, 1758 (1999).
[39] B. Marsen, Phys. Rev. B **60**, 11 593 (1999).
[40] U. Röthlisberger, W. Andreoni, and M. Parrinello, Phys. Rev. Lett. **72**, 665 (1994).
[41] I. Rata, A.A. Shvartsburg, M. Horoi, T. Frauenheim, K.W. Michael Siu, and K.A. Jackson, Phys. Rev. Lett. **85**, 546 (2000).
[42] J.F. Sadoc and N. Rivier, Mater. Sci. Eng., A **294**, 397 (2000).
[43] P. W. Fowler and D. E. Manolopoulos, *An Atlas of Fullerenes* (Oxford, New York, 1995).
[44] R.R. Hudgins, M. Imai, M.F. Jarrold, and P. Dugourd, J. Chem. Phys. **111**, 7865 (1999).
[45] D.E. Bergeron and A.W. Castleman, Jr., J. Chem. Phys. **117**, 3219 (2002).